Carbohydrate Polymers 361 (2025) 123633

Contents lists available at ScienceDirect

Carbohydrate Polymers

journal homepage: www.elsevier.com/locate/carbpol

Characterization of different high amylose starch granules. Part III: How starch fine structures affect retrogradation and formation of type 3 resistant starch

Li Ding [a,b], Jiyu Yang [a], Jacob Judas Kain Kirkensgaard [c,d], Kasper Enemark-Rasmussen [e], Jinhui Chang [a], Lude Zhang [f], Sheng Chen [a], Andreas Blennow [g], Yuyue Zhong [a,*]

[a] Department of Food Science and Nutrition, The Hong Kong Polytechnic University, Hung Hom, Kowloon, Hong Kong, China
[b] Department of Plant and Environmental Sciences, Faculty of Science, University of Copenhagen, Denmark
[c] Department of Food Science, University of Copenhagen, DK-1958 Frederiksberg C, Denmark
[d] Niels Bohr Institute, University of Copenhagen, DK-2100 Copenhagen Ø, Denmark
[e] Department of Chemistry, Technical University of Denmark, DK-2800, Kemitorvet, Building 207 Kgs. Lyngby, Denmark
[f] Xi'an Hengchuang Agricultural Technology Co., Ltd., Weiyang District, Xi'an City, Shaanxi Province, China
[g] Blennow Holding AB, Helsingborg, Sweden

ARTICLE INFO

Keywords:
Starch retrogradation
Resistant starch
Fine structure
Amylose content
Amylopectin

ABSTRACT

The effects of amylose (AM) content (AC) and starch fine structures on the retrogradation and type 3 resistant starch (RS3) formation were investigated using seven starches with various fine structures and ACs ranging from 27 % to 97 %. RS3 contents ranged from 31.9 % to 50.3 %, without a linear increase with AC. However, thermally stable RS3 contents obtained through reheating increased with AC before plateauing at 57 %, ranging from 18.3 % to 39.5 %. Retrograded amylopectin (AP), AM-lipid complexes, and retrograded AM crystals were identified. Notably, as AC reached 57 %, a transition from AP to AM retrogradation was observed. Greater retrogradation degree and structural order induced higher RS3. Retrograded AP, AM-lipid complexes, and retrograded AM were likely composed of AP chains with degree of polymerization (DP) 13–24, AM chains with DP 500–5000, and short AM chains with DP < 500, respectively. RS3 in these HASs comprised a mixture of double-helical and single-helical structures, with their levels likely enhanced by increasing amounts of AM chains with DP < 5000 and AP chains with DP > 36, respectively. These findings provided insights into developing functional foods with desired retrogradation degree and RS3 by controlling AC and fine structures of AM and AP.

1. Introduction

In modern society, an increasing number of people are suffering from diet-related chronic diseases, such as Type 2 diabetes and obesity. Extensive research has shown that the global rise in these conditions is closely linked to the high glycemic index (GI) of foods (Barclay et al., 2008; Heilbronn, Noakes, & Clifton, 2002; Schulze et al., 2004). Starch is the primary glycemic carbohydrate in the human diet, directly influencing insulin secretion and postprandial blood glucose levels (Lafiandra, Riccardi, & Shewry, 2014). Based on its digestion rate and physiological effects, starch can be classified into three categories: rapidly digestible starch (RDS), slowly digestible starch (SDS), and resistant starch (RS). RDS is quickly broken down into glucose, leading to a rapid increase in blood glucose and insulin levels, which is associated with high GI values and increased risk of Type 2 diabetes and obesity (Ramdath et al., 2017). In contrast, RS, a type of dietary fiber, resists hydrolysis in the upper digestive tract and reaches the colon, where it is fermented by gut microbiota to produce short-chain fatty acids with health benefits of preventing diabetes, obesity colon and colon cancer (Zhang, Dhital, & Gidley, 2015). Therefore, the development of starchy foods with higher RS and lower RDS content is crucial for maintaining stable blood sugar levels and promoting gut health.

Various types of RS are proposed by researchers, with type 3 RS (RS3) attracting particular interest due to its high thermal stability and retained nutritional functionality (Haralampu, 2000). RS3 forms during starch retrogradation, a process in which gelatinized amylose (AM) and amylopectin (AP) chains reassociate and recrystallize into a more ordered structure (Luckett & Wang, 2012; Wang, Li, Copeland, Niu, &

* Corresponding author.
E-mail address: yuyuezhong93@163.com (Y. Zhong).

https://doi.org/10.1016/j.carbpol.2025.123633
Received 4 December 2024; Received in revised form 13 April 2025; Accepted 21 April 2025
Available online 23 April 2025

Wang, 2015). Specifically, linear AM chains possessing higher mobility are regarded as the main provider for the short-term (several hours) retrogradation, while the branched AP chains are responsible for the long-term (several days) retrogradation (Park, Baik, & Lim, 2009). As a result, retrogradation can be categorized into AM and AP recrystallization. Moreover, retrograded AM exhibits greater thermal stability (>100 °C) and higher resistance to digestive enzymes compared to retrograded AP (<100 °C), resulting in a greater retention of RS3 after reheating or further processing (Chung & Liu, 2009). Given its stability, RS3 formed by AM retrogradation is particularly suitable for incorporation into processed foods. Therefore, AM molecules play a critical role in enhancing RS3 content and its application.

Starch retrogradation and RS3 are influenced by both AM content (AC) and fine structures of AM and AP. AC is considered a key factor affecting the AP retrogradation degree (Lii, Lai, & Shen, 2004; Yu, Ma, & Sun, 2009), and thereby the RS3 content (You et al., 2022). A study on rice starches with a series of AC (1.1–26.9 %) revealed a non-linear, parabolic relationship between AC and AP retrogradation degree, and found that chain structures of AM and AP, specifically fewer short-medium AM chains and more medium length AP chains were related to increased thermal stability of retrograded AP (Li, Hu, & Li, 2021). Additionally, higher amounts of AP chains with degree of polymerization (DP) 10–39 and/or decreased AM chain length were also reported to elevate the stability and retrogradation degree of recrystallized AP (Gomand, Lamberts, Visser, & Delcour, 2010; Li, Hu, Huang, Gong, & Yu, 2020; Vamadevan & Bertoft, 2018), and more RS3 (Villas-Boas, Facchinatto, Colnago, Volanti, & Franco, 2020). However, previous studies have primarily focused on starches with AC below 40 %, leaving the effects of fine structure and AC at higher levels (> 40 %) largely unexplored. Furthermore, prior research has predominantly examined the less thermally stable retrograded AP, while the mechanisms underlying AM retrogradation remain unclear. Only a few older studies have investigated the influence of AM fine structure on AM retrogradation using synthetic AM chains, likely due to limited availability of starch source with high AC levels. For instance, the perfection of ordered structures in AM chains increased with decreasing chain length for DP values of 250, 110, and 40 after retrogradation (Gidley, 1989). Additionally, the AM aggregation rate was reported to increase with increasing chain length for DP < 110, while it decreased for DP > 250 (Gidley & Bulpin, 1989). Both reports indicated that AM reassociation was largely influenced by its chain length. Natural starch-derived AM exhibits a broad DP range (100−10,000), limiting the applicability of synthetic AM studies to real-world starch retrogradation and RS3 formation.

To address these gaps, we have recently collected high-AM starch (HAS) mutants from diverse crop sources, including potato (high-phosphate-high-amylose potato (HPPS) (Blennow et al., 2005)), maize (NAFU60, Gelose 50 (G50), Gelose 80 (G80) and HylonVI (Tian, Liu, et al., 2024; Zhong et al., 2020)) and barley (amylose only barley starch (AOBS) (Carciofi et al., 2012)). Our previous study on these HASs demonstrated a wide range of AC (34–97 %) and diverse fine structures (Tian, Liu, et al., 2024), making them valuable models for investigating starch retrogradation and RS3 formation. Additionally, digestibility data indicate that RS content in native HASs is more influenced by granular surface structure than by AC alone (Tian, Petersen, et al., 2024). Given the inherent tendency of AM and AP chains to reassociate during retrogradation, we hypothesize that retrogradation degree and RS3 content are primarily determined by fine structural variations rather than AC alone.

Therefore, to investigate how starch fine structure and AC influence retrogradation and RS3 formation, six different HASs with varying fine structures and ACs were used in this study, with normal maize starch (NMS) (Vilpoux & Santos Silveira Junior, 2023) as a control. These starches were fully gelatinized and stored at 4 °C for one day to promote retrogradation, rather than the conventional seven-day storage. This approach was based on the observation that AM is the dominant component in these HASs and undergoes rapid retrogradation within the first 24 h, with extended storage having minimal additional impact (Yu, Xu, Zhang, & Kopparapu, 2014). Thermal properties, helical and crystalline structures as well as *in vitro* digestibility of these retrograded starches were analyzed. Additionally, the thermally stable RS3 contents were also determined by reheating the retrograded starches at 99 °C for 30 mins. Pearson correlation and principal component analysis (PCA) were used to explore the relationships between fine structures/AC and retrogradation properties/RS contents. The findings provide insights into the development of foods with higher RS3 content and offer valuable information for further understanding the molecular mechanisms of AM retrogradation.

2. Materials and methods

2.1. Materials

Seven starches with different ACs and fine structures were used in this study, including NMS, HPPS, G50, HAFU60, G80, Hylon VII and AOBS. For three commercial starches, the NMS (Clinton 106) was kindly provided by Archer Daniels Midland (ADM, Decatur, IL), while the G50 and G80 were from Penford Australia Ltd., NSW, Australia. The HAFU60 and Hylon VII were obtained from Maize Genetic Breeding Laboratory, Northwest A&F University, Yangling, China. The AOBS, generated by RNAi suppressing starch branching enzymes (SBE) from Golden Promise background (Carciofi et al., 2012), was kindly provided by plantCarb ApS, Hørsholm, Denmark. The starches of HAFU60, Hylon VII and AOBS were extracted using alkaline steeping method as reported (Palacios-Fonseca et al., 2013). While, HPPS, a RNAi SBE line based on Dianella background, was prepared as reported in our previous study (Blennow et al., 2005). The apparent AM contents (AACs) determined by the iodine complexation protocol of these starches were 27.4 %, 32.7 %, 44.0 %, 57.0 %, 57.2 %, 69.3 %, and 97.0 %, respectively. Pancreatin from porcine pancreas (Cat. No. P7545, activity 8 × USP), amyloglucosidase (Cat. No. A7095, activity 300 unit/mL) were purchased from Sigma-Aldrich (St. Louis, MO, USA), while isoamylase (EC 3.2.1.68, *E*-ISAMY, 200 units/mL) and pullulanase (E-PULBL, 1000 units/mL) were bought from Megazyme (K-TSTA, Megazyme, Co. Wicklow, Ireland). All other chemicals used in this study were of analytical grade.

2.2. Molecular fine structures

Chain length distributions of the seven debranched native starch samples were analyzed using both size exclusion chromatography (SEC)-triple detector array (SEC-TDA) system (Viscotek, Malvern, UK) and a high-performance anion exchange chromatography with pulsed amperometric detection (HPAEC-PAD) system (Dionex, Sunnyvale, CA, USA). Enzymatic debranching of the starch and chromatographic protocols were as previously reported (Tian, Liu, et al., 2024). For SEC analysis, the separated starch chains were divided into AP and AM, and the AP chains were further segmented into two parts: short AP, DP 6–36 (AP1) and long AP, DP 37–100 (AP2), whereas the AM chains were categorized into three fractions: Short AM with DP 100–500 (AM1), medium AM with DP 500–5000 (AM2), long AM with DP > 5000 (AM3). For HPAEC-PAD, three proportions of side chains were categorized: fa (DP 6–12), fb_1 (DP 13–24), fb_2 (DP 25–36), and fb_3 (DP > 36) chains.

2.3. Preparation of retrograded starches

Starch granules (4.0 g) were suspended in 36 mL of MilliQ water. To reach full gelatinization, the NMS and HPPS suspensions were incubated in a water bath at 99 °C for 45 min, while starch suspensions for G50, G80, HAFU60, Hylon VII and AOBS were heated in an oil bath at 140 °C for 45 min. After cooling to ambient room temperature, the starch pastes were placed at 4 °C for 1 day. All retrograded products were snap-frozen in liq N_2, lyophilized and gently milled and stored dry prior to further

use.

2.4. In vitro digestibility of retrograded and reheated starches

The *in vitro* digestion of both retrograded and reheated starch samples was analyzed as reported (Zhang, Huang, Luo, & Fu, 2012) with modifications. Twenty mg of retrograded starch samples were incubated in 1 mL 50 mM sodium acetate buffer (pH 5.2) with 5 mM calcium chloride at 37 °C for 30 min. To mimic daily boiling cooking, the retrograded starch suspensions were reheated at 99 °C for 0.5 h before the 37 °C incubation. Next, 1 mL sodium acetate buffer containing 33.36 × USP pancreatin and 1.4 U amyloglucosidase were added to both non-reheated and reheated starch solutions to initiate the digestive process. After 20 and 120 mins, 100 μL of digestive solution were taken out and immediately mixed with 1 mL of 96 % aqueous ethanol to terminate the reaction. The amount of released glucose in the supernatant was quantified spectrophotometrically with the GOPOD kit (K-GLUC; Megazyme). Rapidly digestible starch (RDS), slowly digestible starch (SDS) and resistant starch (RS) were quantified as reported in (Zhang et al., 2012).

2.5. Differential scanning calorimeter (DSC)

The thermal properties of retrograded starch samples were measured by a DSC 1 (Mettler Toledo, Schwerzenbach, Switzerland) instrument. Starch (5 mg, dry basis) were weighed into medium-pressure stainless-steel crucibles, and 15 μL of MilliQ water was added, followed by sealing and equilibration at 4 °C overnight. For measurements, the pans were heated from 30 to 180 °C with a heating rate of 10 °C per min using an empty pan as reference.

2.6. Solid-state ^{13}C nuclear magnetic resonance (NMR) spectroscopy

The helical structures of retrograded starches were estimated by ^{13}C NMR spectroscopy, performed at ^{13}C frequency of 150.9 MHz using a Bruker AV-600 spectrometer, as previously described (Ding et al., 2023). The raw NMR spectra were decomposed into respective amorphous and ordered sub-spectra by subtracting the spectra of amorphous references at about 85 ppm, and the relative amounts of single helices (102–103 ppm), double helices (99–101 ppm), and amorphous regions were calculated separately (Tan, Flanagan, Halley, Whittaker, & Gidley, 2007).

2.7. Wide-angle X-ray scattering (WAXS)

A Nano-inXider instrument (Xenocs SAS, Grenoble, France) equipped with a Cu Kα source with a 1.54 Å wavelength and a two-detector setup was used to analyze the crystalline long-range orders of retrograded starches (Zhong et al., 2021). After moisture equilibration in at relative humidity of 90 % for 1 week, starch samples were analyzed using the parameters as previously reported (Ding et al., 2023), and the relative contents of B- and V- type crystalline allomorphs and total relative crystallinities were calculated.

2.8. Fourier transform infrared (FTIR) spectroscopy

The short-range molecular order of retrograded starches was estimated using a Bomem MB100 FTIR spectrometer (ABB-Bomem, Quebec, Canada) equipped with an attenuated total reflectance (ATR) single reflectance cell with a diamond crystal. The starch powder samples were scanned 64 times over the range of 4000–600 cm^{-1} at a resolution of 8 cm^{-1} against air. The ratio of absorbance at 1047 cm^{-1} to that at 1022 cm^{-1} (A_{1047} / A_{1022}) was calculated to represent the surface short-range order.

2.9. Statistical analysis

Experiments were performed at least in triplicates, and the results were expressed as means ± standard deviations. In case of the ^{13}C NMR, one measurement was performed. Statistically significant differences ($p < 0.05$) were analyzed by Analysis of Variance (ANOVA) followed by Duncan's test. Statistical analysis and Pearson correlation analysis were conducted by the SPSS 25.0 software (SPSS, Inc. Chicago, IL, USA). While, the PCA analysis using the partial least squares regression was conducted by SIMCA 14.0 software (Guo et al., 2024).

3. Results and discussion

3.1. Chain length distributions

Chain length distributions determined by SEC and HPAEC-PAD were shown in Table S1 and Table S2, respectively. Our previous study on these HASs comprehensively reported and discussed their fine structures (Tian, Liu, et al., 2024). To avoid duplication, the current study only discussed the AM fine structures, which were not characterized in (Tian, Liu, et al., 2024). AM were divided into three fractions, short AM1 with DP < 500, medium AM2 with DP 500–5000, and long AM3 with DP > 5000. The average chain length (ACL) of AM1 (ACL_{AM1}) ranged from 310.1 DP to 318.6 DP, with NMS and G50 being the highest and HPPS being the lowest. The ACL_{AM2} and ACL_{AM3} of AOBS were the highest (1731.2 DP and 10,745.1 DP, respectively). The relative content (RC) of AM1 (RC_{AM1}), AM2 (RC_{AM2}) and AM3 (RC_{AM3}) ranged 5.4 % - 13 %, 11.8 % - 38.5 %, and 0.8 % - 34.2 %, respectively. NMS presented the lowest three RCs, while Hylon VII had the highest RC_{AM1} and AOBS exhibited the highest RC_{AM2} and RC_{AM3}.

3.2. In vitro digestibility of retrograded and reheated starches in HASs

As retrograded starch is categorized as RS3 (Ma, Hu, & Boye, 2020), *in vitro* digestibility, including the relative contents of RDS, SDS and RS of retrograded starches, was measured (Table 1). G80 and AOBS presented the highest RS3 (~50 %), followed by Hylon VII (48 %), NAFU60 and HPPS (~43 %), and G50 (38 %), all higher than the NMS control (32 %). However, in contrast to earlier studies and traditional notion of higher AAC inducing more RS3, no linear increasing trend for the RS3 with increasing AAC was observed in this study. These results indicated that except AAC, there are supposedly other factors mainly affecting RS3, such as the fine structures of AM and/or AP (Dobosz et al., 2019). This was further supported by significantly different RS3 contents between two HASs (NAFU60 and G80) with similar AACs (~57 %). However, NAFU60 had higher AAC but similar RS3 to HPPS, further indicating the fine structures might have larger effects than AAC.

Retrograded foods, having rigid or toughened structure, are usually reheated before consumption (Han, Kim, Lee, & Rhee, 2009), decreasing RS and increasing RDS contents. To evaluate the amount of thermally stable RS3 after reheating (e.g. reheated RS3), these retrograded starches were reheated at 99 °C for 30 min to mimic a daily boiling procedure (Karunarathna et al., 2024). The digestibility data (Table 1) demonstrated that the reheated RS3 ranged from 18.3 % to 39.5 %, following the order: G80 ~ Hylon VII > AOBS > NAFU60 > HPPS~G50 > NMS. Additionally, the reheated RS3 increased with increasing AAC and then plateaued as the AAC reached 57 %. These findings suggested that AAC is a crucial factor influencing the amount of RS3 in cooked, reheated starch systems when AAC is lower than 57 %. This is reasonable as mainly AM crystals withstand 99 °C of reheating, and therefore resist the amylolytic attack during digestion (Chung & Liu, 2009). At AAC > 57 %, the plateau observed in reheated RS3 levels is likely due to the saturation of AM recrystallization, whereby additional AM molecules are unable to form more crystals under the given conditions.

Table 1
RDS, SDS, and RS contents of retrograded and reheated high amylose starches[1].

Samples	Retrograded			Reheated		
	RDS[2] (%)	SDS (%)	RS (%)	RDS (%)	SDS (%)	RS (%)
NMS	59.6 ± 1.8^{a}	8.5 ± 0.4^{c}	31.9 ± 1.1^{e}	64.6 ± 0.5^{b}	17.1 ± 3.3^{a}	18.3 ± 2.9^{e}
HPPS	48.5 ± 0.8^{c}	8.1 ± 1.2^{c}	43.1 ± 1.1^{c}	69.6 ± 0.4^{a}	5.0 ± 0.1^{d}	25.3 ± 0.3^{d}
G50	50.9 ± 1.3^{b}	11.2 ± 1.4^{b}	37.9 ± 0.4^{d}	63.2 ± 0.4^{c}	11.1 ± 0.8^{b}	25.7 ± 0.5^{d}
NAFU60	48.0 ± 1.8^{c}	9.0 ± 1.5^{c}	43.0 ± 0.7^{c}	59.5 ± 1.1^{d}	8.7 ± 0.7^{c}	31.8 ± 0.6^{c}
G80	36.1 ± 1.8^{e}	13.6 ± 2.6^{a}	50.3 ± 0.9^{a}	58.2 ± 0.6^{e}	2.2 ± 0.4^{e}	39.5 ± 0.5^{a}
Hylon VII	42.9 ± 1.2^{d}	9.1 ± 0.9^{c}	48.0 ± 0.5^{b}	57.9 ± 0.6^{e}	3.1 ± 0.4^{e}	39.1 ± 0.3^{a}
AOBS	46.3 ± 1.6^{c}	4.1 ± 1.1^{d}	49.7 ± 1.2^{ab}	55.9 ± 1.1^{f}	7.0 ± 1.7^{c}	37.0 ± 1.4^{b}

[1] Values are means ± SD. Values with different letters in the same column are significantly different at $p < 0.05$.
[2] RDS: rapidly digestible starch; SDS: slowly digestible starch; RS: resistant starch.

3.3. Thermal properties of retrograded HASs

As both AM and AP can retrograde during cooling and storage, thermal temperatures (T_o, T_p and T_c) determined by DSC were used to distinguish the AM (melting temperature > 100 °C) and AP (< 80 °C) retrogradations (Ding, Zhang, Tan, Fu, & Huang, 2019). DSC results (Table 2) indicated that retrograded NMS and HPPS exhibited only one peak (Peak I) with a thermal temperature range 40–80 °C, suggesting unwinding and melting of double helical segments formed solely by retrograded AP (Ding et al., 2019). In contrast, other retrograded HASs displayed two peaks. Besides a lower temperature peak designated Peak I, G50 had a second peak (Peak II) melting in the 80–110 °C, similar to the melting temperature range (90–110 °C) of AM-lipid complex existing in the non-defatted starches (Zhang et al., 2012). Thus, Peak II probably corresponded to the melting of single helices generated by AM-lipid complex. Interestingly, a third peak (Peak III) at even higher temperatures (130–160 °C) was found in NAFU60, G80, Hylon VII, and AOBS, all with AAC higher than 57 %, attributed to the melting of double helices from retrograded AM. Recrystallized AM is more thermally stable than the retrograded AP (Ding et al., 2019). To summarize, as AAC increased, these HASs transitioned from AP to AM retrogradation when AAC reached 57 % after one day of storage at 4 °C. To the best of our knowledge, this is the first report identifying the AAC threshold that distinguishes AP from AM retrogradation under the condition used.

The enthalpy change (ΔH) detected by DSC is associated with the number of crystals formed during retrogradation, which can represent the retrogradation degree (Karim, Norziah, & Seow, 2009; Wang et al., 2015). Among AP retrograded starches, HPPS had the highest ΔH, followed by NMS, while G50 had the lowest value. Thus, the retrogradation degree for AP first increased and then decreased with increasing AAC from 27 % to 44 %, consistent with their RS3 contents. Combined with the absence of AP retrogradation at AAC > 57 %, these findings suggest that increasing AAC from 27 % - 97 % initially promotes, subsequently limits, and ultimately inhibits AP retrogradation under the conditions used. Except for the retrograded AP, G50 presented 1.3 J/g of AM-lipid complex. The lower AP retrogradation degree of G50 compared to NMS is likely attributed to the presence of AM-lipid complex retarding the starch reorganization (Becker, Hill, & Mitchell, 2001). In addition, among AM retrograded HASs, AOBS had the highest ΔH for the AM-lipid crystals (2.7 J/g), followed by Hylon VII (1.7 J/g) and NAFU60 (1.2 J/g), while that of G80 was the lowest (1.0 J/g). These results showed a decreased and then increased trend in the amount of AM-lipid crystals as AAC increased from 44 % to 97 %. For the retrograded AM crystals (Peak III), G80 (1.3 J/g), AOBS (1.2 J/g) and Hylon VII (0.9 J/g) had higher retrogradation degrees than NAFU60 (0.7 J/g), in line with their RS3 contents. These data demonstrated that the higher retrogradation degree of either AM or AP enhanced the RS3 contents (Villas-Boas et al., 2020). No significant difference in the ΔH of Peak III with melting temperatures above 99 °C of reheating, likely implied the saturation of AM recrystallization and explained the plateau of reheated RS3 contents when AAC was higher than 57 %. These observations indicated that the degrees of AP and AM retrogradation were at least partly independent on AAC, and additional factors are involved in affecting the retrogradation behaviors of HASs, supporting our hypothesis. Notably, although AP retrograded HASs showed higher ΔHs than those of AM retrograded HASs, they presented lower RS3 contents, further demonstrating greater enzymatic resistance of retrograded AM compared to AP (Chung & Liu, 2009). Interestingly, the total ΔH of both Peak II and Peak III increased

Table 2
Thermal properties of retrograded high amylose starches[1].

Samples	Peak I				Peak II			
	T_o [2](°C)	T_p (°C)	T_c (°C)	ΔH (J/g)	T_o (°C)	T_p (°C)	T_c (°C)	ΔH (J/g)
NMS	41.2 ± 2.1^{b}	53.0 ± 1.1^{b}	66.6 ± 2.7^{b}	2.8 ± 0.3^{ab}	n.d.[3]	n.d.	n.d.	n.d.
HPPS	44.9 ± 1.7^{a}	60.5 ± 0.6^{a}	81.5 ± 2.2^{a}	3.3 ± 0.1^{a}	n.d.	n.d.	n.d.	n.d.
G50	45.7 ± 0.2^{a}	61.6 ± 1.4^{a}	79.5 ± 0.3^{a}	2.3 ± 0.2^{b}	86.9 ± 0.3^{a}	100.5 ± 0.0^{b}	110.9 ± 1.0^{a}	1.3 ± 0.1^{c}
NAFU60	n.d.	n.d.	n.d.	n.d.	86.9 ± 0.4^{a}	101.3 ± 0.1^{a}	110.5 ± 0.5^{a}	1.2 ± 0.0^{c}
G80	n.d.	n.d.	n.d.	n.d.	85.7 ± 2.2^{a}	96.7 ± 1.7^{c}	107.7 ± 0.5^{a}	1.0 ± 0.0^{d}
Hylon VII	n.d.	n.d.	n.d.	n.d.	82.3 ± 0.6^{b}	97.4 ± 0.0^{c}	107.7 ± 0.3^{a}	1.7 ± 0.0^{b}
AOBS	n.d.	n.d.	n.d.	n.d.	87.5 ± 0.0^{a}	95.7 ± 0.2^{c}	102.4 ± 0.8^{b}	2.7 ± 0.5^{a}
Samples	Peak III				ΔH_ II + ΔH_ III (J/g)			
	T_o (°C)	T_p (°C)	T_c (°C)	ΔH (J/g)				
NMS	n.d.	n.d.	n.d.	n.d.	n.d.			
HPPS	n.d.	n.d.	n.d.	n.d.	n.d.			
G50	n.d.	n.d.	n.d.	n.d.	1.3			
NAFU60	144.8 ± 1.7^{a}	152.3 ± 2.9^{a}	161.1 ± 0.9^{a}	0.7 ± 0.0^{b}	1.9			
G80	138.7 ± 0.1^{b}	147.2 ± 0.6^{b}	158.7 ± 1.1^{b}	1.3 ± 0.3^{a}	2.3			
Hylon VII	145.3 ± 0.7^{a}	151.7 ± 0.3^{a}	158.6 ± 0.0^{b}	0.9 ± 0.2^{ab}	2.6			
AOBS	134.0 ± 2.9^{c}	147.1 ± 1.2^{b}	155.6 ± 0.5^{c}	1.2 ± 0.3^{a}	3.9			

[1] Values are means ± SD. Values with different letters in the same column are significantly different at $p < 0.05$.
[2] T_o: onset melting temperature; T_p: peak melting temperature; T_c: conclusion melting temperature; ΔH: melting enthalpy change.
[3] n.d. = not detectable.

with rising AAC, indicating a dependence of AAC. This trend is attributed to that the higher AAC facilitate greater recrystallization (Li et al., 2021) and form more single helices with endogenous lipids (Chang, He, & Huang, 2013).

3.4. Structural ordering of retrograded HASs

Linear AM chains and side chains of AP tend to form double helices during retrogradation, and these double helices further pack and align into crystals, thereby forming a more ordered structure (Chang, Zheng, Zhang, & Zeng, 2021; Klucinec & Thompson, 1999; Li et al., 2021). Crystallinity as calculated from the WAXS profiles reflects the overall order of starch crystals, including the amount, packing and alignment of double helices, as recognized as long-range order (Lu, Tian, & Ma, 2023). Short-range order can be estimated from the FTIR ratio of absorbances at 1047 cm^{-1} to at 1022 cm^{-1} (A_{1047}/A_{1022}), representing bonding order related to the arrangement of double helices on the starch surface (Tian, Liu, et al., 2024).

The WAXS profiles of retrograded HASs (Fig. 1), demonstrated that all retrograded starches presented a B-type crystalline allomorph, typical for the retrograded starches (Ding et al., 2019; Xu et al., 2012; Zhu, Zhan, Chen, & Tian, 2020). Additionally, the peak at 2θ of 20° for these starches was assigned to the endogenous AM-lipid complex to produce single-helical "V-type" crystalline polymorphs (Wang, Wang, Guo, Liu, & Wang, 2017). As shown in Table 3, with increasing AAC, both AP (NMS, HPPS and G50) and AM (other HASs) retrograded starches presented an increased and then decreased trend in ordered degrees of double helices, B-type crystallinity and A_{1047}/A_{1022}, generally in line with retrogradation degree results. Thus, the ordered degrees, primarily influenced by retrogradation degree, were also modulated by AAC and additional structural factors. Additionally, these trends in ordered degrees also closely followed changes in RS3 contents, aligning with the well-established role of structural order in reducing amylolytic digestibility (Zhang et al., 2015). Therefore, greater retrogradation degree induced higher perfection of structural order, thereby forming more RS3. However, the opposite trend between AM-lipid crystals (Table 2, Peak II) and structural order further suggested that AM-lipid complexes acted as crystalline defects (Zhong et al., 2020) or limited the extent of retrogradation to reduce the structural order. This interpretation was further supported by the low ordered degrees of double helices and A_{1047}/A_{1022} observed in G50 with a high content of AM-lipid complexes, even lower than NMS. Furthermore, single-helical content and V-type crystallinity exhibited a general increasing trend with AAC, demonstrating AAC dependence. This effect is attributed to the ability of AM to form single helices with endogenous lipids (Ding et al., 2019).

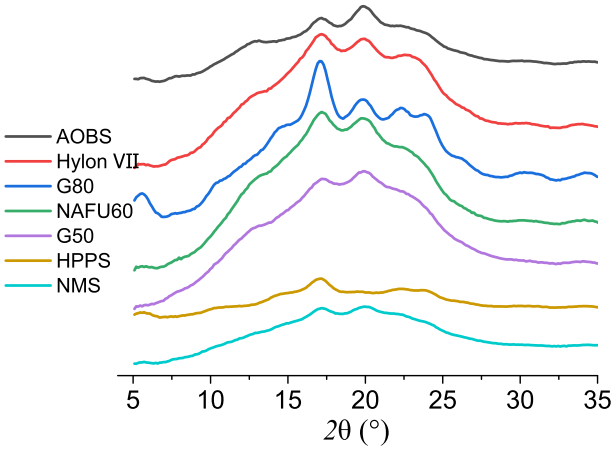

Fig. 1. WAXS diffractograms of retrograded high amylose starches.

3.5. Understanding how the fine structures of HAS affects starch retrogradation and RS3 by Pearson correlation and PCA analysis

The structure-property analysis in our study revealed a positive correlation between RS3 content and the degree of structural order, with both parameters being influenced by the extent of retrogradation. Furthermore, these three parameters were more significantly affected by other structural factors than by AAC. To identify the key structural factors controlling these parameters, we performed Pearson correlations (Fig. 2) and PCA (Fig. 3) between the fine structure data (Table S1 and Table S2) and retrogradation properties (Sections 3.2 to 3.4). Although multiple previous studies reported the relationships between fine structure of AM and AP and starch properties, the present study specifically focused on starch retrogradation using a series of HASs as materials. The correlations related to AP retrogradation can confirm or supplement findings from previous studies (Gong, Cheng, Gilbert, & Li, 2019; Li et al., 2020; Vamadevan & Bertoft, 2018). However, this study is the first to investigate the correlations involving AM-lipid complexes, AM retrogradation, and reheated RS3, providing novel insights into mechanisms of AM retrogradation and RS3 formation.

3.5.1. Retrograded AP (DSC Peak I)

T_o and T_p of Peak I (T_o_I and T_p_I) positively correlated with the average chain length (ACL) of the AP2 chains (ACL_{AP2}), ACL_{fa} and ACL_{fb3}, but negatively correlated with the relative content (RC) of the AP1 chains (RC_{AP1}) and RC_{fa} (Fig. 2), consistent with the clustering of T_p_I with RC_{AP1} in PCA analysis (Fig. 3). These data indicated that longer AP chains, especially those with DP > 36 elevated the thermal stability of AP crystals, while higher amount of AP chain with DP 6–36 (especially fa chains with DP 6–12) reduced their thermal stability, consistent with previous reports (Li et al., 2021; Vamadevan & Bertoft, 2018). During cooling and storage at 4 °C, the adjacent AM and/or AP chains dispersed in the starch paste re-associate via hydrogen bonds to form double helices, and these double helices further aggregate and pack together into crystallites (Vamadevan & Bertoft, 2018). AP chains with DP < 10 cannot form double-helices with themselves, but may co-crystallize with other longer chains (Gidley & Bulpin, 1987; Grewal et al., 2015). Additionally, longer AP side chains are believed to have sufficient flexibility and mobility to form longer and more stable double helices (Li et al., 2021; Li & Zhu, 2017). Related to this, T_c_I was significantly and positively correlated with RC_{fb2}, indicating that more AP chains with DP 25–36 enhanced the thermal stability of the most perfect AP crystals. However, ΔH_I displayed a weak negative correlation with RC_{fb3} but positive correlation with RC_{fb1}, likely suggesting that fewer AP chains with DP > 36 and more AP chains with DP 13–24 are capable of forming more AP crystals (Vandeputte, Vermeylen, Geeroms, & Delcour, 2003). Although long AP side chains favors forming long and stable helices, our data shows that the retrograded AP double helices might be mainly formed by short AP chains with DP 13–24. Gomand et al. (2010) also reported that AP chains with DP 18–25 positively correlated with the retrogradation enthalpy. The clustering of ΔH_I with RC_{AP1} and RC_{fb1} from PCA analysis in Fig. 3 further confirmed that the retrograded AP double helices were composed of short AP with DP 6–36, especially those with DP 13–24.

3.5.2. AM-lipid complexes (DSC Peak II)

T_o_II, T_p_II and T_c_II only presented weak positive correlations with ACL_{AM1}, and negative correlations with AAC and RC_{AM}, indicating that longer AM1 chains with DP < 500, and less content of AM contributed to enhanced thermal stability of the AM-lipid complexes. ΔH_II positively highly correlated with ACL_{AM2} and RC_{AM3}, and weakly with RC_{AM2} and ACL_{AM3}, further indicating that AM-lipid complexes were predominantly formed by longer AM chains (AM2 and AM3 with DP > 500). PCA results in Fig. 3 confirmed these correlations by clustering of ΔH_II with RC_{AM}, AAC, RC/ACL_{AM2} and RC/ACL_{AM3}. Previous research also reported an increase in ΔH for AM-lipid complexes with increasing AM

Table 3
The relative contents of double-helix, single-helix, and amorphous regions derived from spectra of ^{13}C NMR, B/V type crystallinity from WAXS, and FTIR ratio of absorbance at 1047/1022 cm^{-1}(A_{1047}/A_{1022}) of retrograded high amylose starches[1].

Samples	^{13}C NMR			WAXS			FTIR A_{1047}/A_{1022}
	Double helix (%)	Single helix (%)	Amorphous (%)	B-type crystallinity (%)	V-type crystallinity (%)	Total crystallinity (%)	
NMS	6.2	0.8	93.0	5 ± 0^{d}	1 ± 0^{e}	6 ± 0^{e}	0.51 ± 0.01^{b}
HPPS	16.1	4.9	79.0	16 ± 1^{b}	1 ± 0^{e}	17 ± 1^{b}	0.59 ± 0.03^{a}
G50	4.5	5.5	90.0	7 ± 0^{c}	2 ± 0^{de}	9 ± 1^{d}	0.49 ± 0.01^{c}
NAFU60	6.6	6.4	87.0	8 ± 0^{c}	5 ± 0^{bc}	13 ± 1^{c}	0.50 ± 0.00^{bc}
G80	19.2	9.8	71.0	19 ± 1^{a}	3 ± 1^{d}	22 ± 2^{a}	0.59 ± 0.00^{a}
Hylon VII	15.0	5.0	80.0	9 ± 0^{c}	4 ± 0^{c}	13 ± 0^{c}	0.52 ± 0.02^{b}
AOBS	11.9	8.1	80.0	8 ± 0^{c}	8 ± 0^{a}	16 ± 0^{b}	0.57 ± 0.01^{a}

[1] Values are means ± SD. Values with different letters in the same column are significantly different at $p < 0.05$.

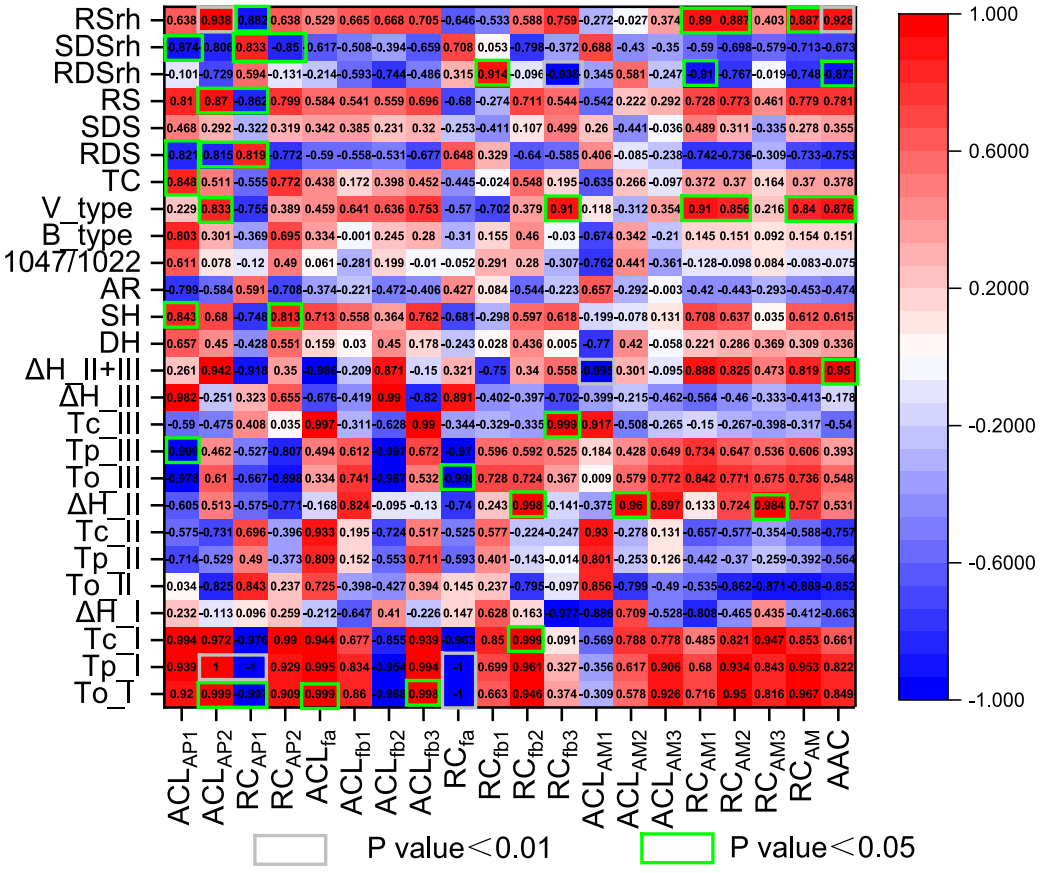

Fig. 2. Pearson correlation coefficients between fine structural parameters and properties of retrograded high amylose starches (ACL_X: average chain lengths (DP) of fraction X; RC_X: relative amount of fraction X; AP1: short amylopectin chains with DP 6–36; AP2: long amylopectin chains with DP 37–100; fa, amylopectin chains with DP 6–12; fb1: amylopectin chains with DP 13–24; fb2 amylopectin chains with DP 25–36; fb3: amylopectin chains with DP > 36: AM1: short amylose chains with DP 100–500; AM2: medium amylose chains with DP 500–5000; AM3: long amylose chains with DP >5000; AAC: apparent amylose content; T_o: onset melting temperature; T_p: peak melting temperature; T_c: conclusion melting temperature; ΔH: melting enthalpy change; I, II, III: DSC Peak I, Peak II and Peak III; SH: relative content of single helices; DH: relative content of double helices; AR: relative content of amorphous region; TC: total crystallinity; B-type: B-type crystallinity; V-type: V-type crystallinity; RDS, SDS and RS: rapidly digestible starch, slowly digestible starch and resistant starch of retrograded starches; RDS_{rh}, SDSrh and RS_{rh}: rapidly digestible starch, slowly digestible starch and resistant starch of reheated starches.)

chain length, with peak DP ranging from 20 to 950 at a complexation temperature of 90 °C (Gelders, Vanderstukken, Goesaert, & Delcour, 2004). Longer AM chains had the potential to form longer and larger amounts of single helices with lipids (Gelders, Duyck, Goesaert, & Delcour, 2005). Interestingly, ΔH_II also had a significant positive correlation with RC_{fb2}, implying that the long AP side chains with DP 25–36 likely co-align with these AM-lipid single helices or directly form complexes with lipids (Castro-Campos et al., 2024).

3.5.3. Retrograded AM (DSC Peak III)

Notably, T_o_III and T_p_III exhibited notable negative correlations with ACL_{AP1} and RC_{fa}. These data suggested that longer AP chains with DP 6–36 and more AP short chains with DP 6–12 likely restricted the mobility and the packing of retrograded AM double helices, due to the dilution effect and steric hindrance (Sievert & Wursch, 1993). In addition, T_c_III displayed a strong positive correlation with RC_{fb3}, indicating that AP chains with DP > 36 supported stabilizations of these retrograded AM crystals (Bertoft, 2017). Additionally, ΔH_III showed only weak positive correlations with ACL_{AP1} and ACL_{fb2}, indicating that

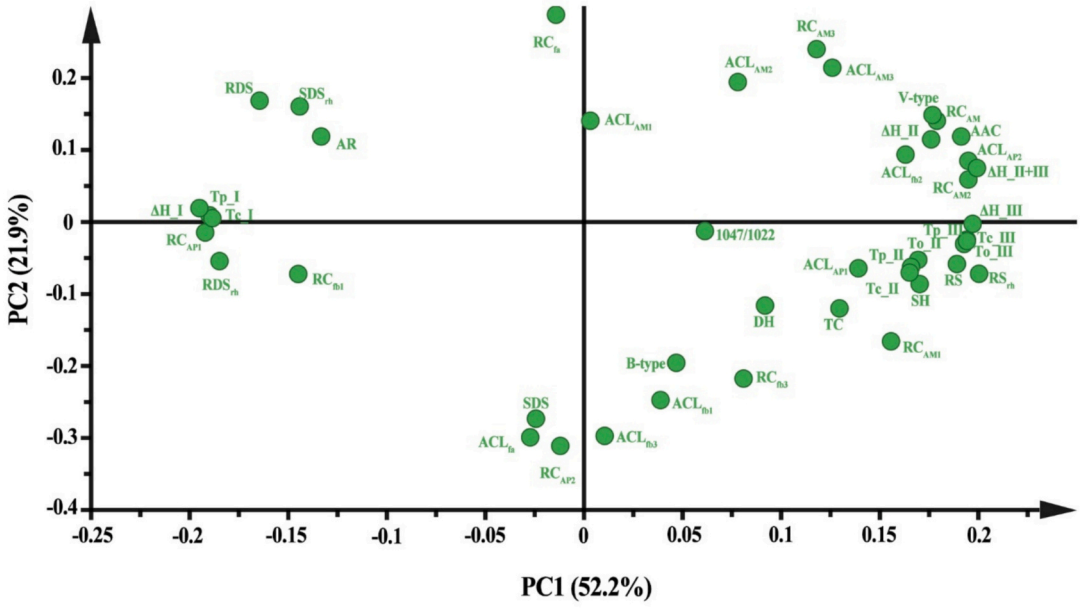

Fig. 3. Principal component analysis (PCA) on the fine structural parameters and retrogradation properties of high amylose starches (All abbreviations are the same as in Fig. 2).

longer AP chains of DP 6–36, especially those with DP 25–36, promoted the formation of retrograded AM helices. PCA analysis also showed clustering of T_o_III, T_p_III, T_c_III and ΔH_III with ACL_{AP1} and RC_{fb3}. These results indicated that, to some extent, AP fine structures affected the formation of retrograded AM crystals. Moreover, the weak positive correlations between T_c_III and ACL_{AM1}, as well as T_o_III or T_p_III and RC_{AM1} suggested that longer, and a higher proportion of short AM chains with DP < 500 increased the thermal stability of these retrograded AM crystals, consistent with clustering of T_o_III, T_p_III or T_c_III with RC_{AM1} (Fig. 3). As retrograded AM is only a part of AM crystals, it is reasonable that the ΔH_III for this fraction did not significantly correlate with AAC or AM fine structures. This is further supported by the strong positive correlations found between the ΔH_II + III and AAC and RC_{AM} (mainly AM1 and AM2), which reflected that retrograded AM and AM-lipid complexes were primarily composed of short and medium AM chains with DP < 5000. Combining the Pearson correlations of ΔH_II with RC_{AM2}, these results implied that the retrograded AM crystals (ΔH_III) were likely composed of short AM1 chains with DP < 500, as evidenced by the clustering of ΔH_III with RC_{AM1} in PCA analysis. This finding provides the first evidence on the main component of retrograded AM under the condition used. Additionally, the negative relationship found between ΔH_II + III and ACL_{AM1} indicated that the shorter the AM chains with DP < 500, the more AM crystals were formed, attributed to the high mobility and flexibility of such short AM chains (Chung & Liu, 2009). A previous study also reported that the AM aggregation rates decreased with increasing chain length for chains with DP > 250 at >1 % concentration (Gidley & Bulpin, 1989).

3.5.4. Ordered degrees in helical, short-range and long-range structures

Double helical content, short-range order (A_{1047}/A_{1022}), and B-type- and total crystallinity showed positive correlations with ACL_{AP1} and RC_{AP2} (Fig. 2). Additionally, these order degrees clustered together with ACL_{AP1} and RC_{fb3} (Fig. 3). Longer chain length of AP chains within the DP 6–36 pool and more AP chains with DP > 36 therefore likely favored higher ordered degrees during retrogradation. Longer AP chains among the DP 6–36 chains, especially those with DP 13–24, has the capability to form longer and more double helices, thereby producing more stable crystals (Li et al., 2021). Moreover, AP chains with DP > 36 can serve as strong backbone for these helices to pack and align, thereby stabilizing these double helices and increasing their thermal stability (Bertoft, 2017), as discussed in the retrograded AP section. Additionally, these ordered degrees also negatively correlated with ACL_{AM1} and clustered with RC_{AM1}, indicating that shorter AM1 chains with DP < 500 supported the formation of higher structural order (Gidley, 1989). Short AM1 chains with DP < 500 constituted retrograded AM crystals, as discussed above, and the perfect packing of double helices in these AM crystals increased the ordered degrees. However, these correlations, as discussed above, were weak, and no significant correlations were detected between the ordered structures and AAC/fine structures. The ordered structures were perhaps controlled by combined effects of AAC and fine structures (Zhang et al., 2024), and thus single parameters alone do not sufficiently explain the variations in these ordered structures. Single helical content (weakly) and V-type crystallinity (strongly) were both positively correlated with AAC and RC_{AM} (mainly RC_{AM1} and RC_{AM2}), suggesting that a higher relative content of AM chains, especially those with short and medium lengths (DP < 5000), contributed to more single helices capable of forming V-type crystalline entities. These Pearson correlations were confirmed by PCA clustering of V-type crystallinity and the single helical content with the RC_{AM2} and RC_{AM1}, respectively. Combining the main components of Peak II (AM2 and AM3), we concluded that the AM-lipid helical structure consisted at least of AM2 chains with DP of 500–5000, providing new insights into the formation of AM complexes with endogenous lipids. The Short and medium AM chains were reported to be the main contributors of single helices of native HASs (Tian, Liu, et al., 2024). These single helices supposedly melted during heating and then reformed during cooling and storage, especially those medium AM2 chains. They also showed positive correlations with ACL_{AP2}, RC_{fb3} and RC_{AP2}, indicating that a higher proportion of longer AP chains with DP > 36 promoted the formation of AM-lipid complexes.

3.5.5. In vitro digestibility of retrograded starches

After retrogradation, RS significantly and positively correlated with ACL_{AP2}, and negatively correlated with RC_{AP1}, as opposed to the positive correlations with retrograded RDS. In addition, RS (positively) and RDS (negatively) correlated weakly with ACL_{AP1} and RC_{AP2}. In PCA analysis, the retrograded RS also clustered with ACL_{AP1} and RC_{fb3} (Fig. 3). These results suggested that longer AP chains and a higher proportion of AP chains with DP > 36 are associated with increased RS3 but decreased RDS after retrogradation, consistent with the positive correlation of RS

with AP long chains (DP 20–210) as reported (Luckett & Wang, 2012). As discussed earlier, longer AP chains and more AP chains with DP > 36 are related to more single helices and higher ordered degrees. Single helices formed chiefly by AM-lipid complexes are categorized into the so-called type 5 RS (RS5), presenting compact and stable structures (Gutiérrez & Tovar, 2021). Additionally, highly ordered structures resulting from perfect packing of double helices, typically as the B-type crystalline allomorph, formed by retrograded AP and/or AM can reduce enzyme accessibility during digestion (Ma et al., 2020; Zhang et al., 2015). Our study further emphasized that the RS3 derived from these retrograded HASs is a mixture, specifically a narrow sense combination of RS3 (double-helical aggregates) and RS5 (single-helical lipid complex aggregates), supported by the clustering of RS with ΔH_III and SH (Fig. 3). In this manuscript, unless otherwise specified, RS3 refers to RS in retrograded starches in the broad sense, encompassing both double-helical aggregates and single-helical lipid complex aggregates. The highest content of RC_{AP2} of HPPS (33.4 %) was likely the primary factor contributing to its highest structural order, and, consequently, the highest RS3, among AP retrograded starches. However, we observed only weak positive correlations between RS and AAC/RC_{AM} (particularly with RC_{AM1} and RC_{AM2}), and clustering of RS with RC_{AM1}. Short and medium AM chains with DP < 5000 were the main component of AM single and double helices, thereby increasing the enzymatic resistance. Gong et al. (2019) also revealed the possibility of AM short-medium chains forming crystalline structures resistant to digestion.

3.5.6. *In vitro digestibility of reheated starches*

Interestingly, the positive correlation between the RS and AAC/RC_{AM} was strengthened after reheating, demonstrating that thermally stable RS3 is AAC dependent. Among AM chains, the fraction RS_{rh}, i.e. reheated RS3, predominantly and positively correlated with RC_{AM1} and RC_{AM2} (Fig. 2), and clustered with RC_{AM1} (Fig. 3), Short AM1 and medium AM2 chains formed AM double helices as well as single helices as discussed above, which remained after reheating at 99 °C (Haralampu, 2000). Therefore, our study highlighted that reheated RS3 also consisted of a mixture of double-helical and single-helical aggregates, formed by short and medium AM chains with DP < 5000. This finding explains the higher RS3 contents in Hylon VII and AOBS compared to NAFU60, as their combined contents AM1 and AM2 chains were 45.3 %, 47.4 %, and 40.4 %, respectively (Table S1). RS_{rh} also positively correlated with ACL_{AP2} and negatively related to RC_{AP1}. AP2 chains with DP > 36 enhanced the thermal stability of AM double helices and elevated degrees of order, thereby retaining more RS3 after reheating. The highest RS3 contents of G80 was thus probably attributed to its high content of AP2 (32.6 %) chains and medium high content of both AM1 and AM2 (38.3 %). Related to the AM chains, RDS_{rh} negatively correlated with AAC and RC_{AM} (mainly RC_{AM1}), indicating that more AM chains, especially short AM chains with DP < 500, were related to less RDS after reheating. Short AM chains were the main component of the AM double helical segments with highly enzymatic and thermal resistance, thereby decreasing the reheated RDS. Additionally, positive correlation and clustering with RC_{fb1} was observed for RDS_{rh}, further suggesting that the RDS_{rh} was mainly formed by AP chains with DP 13–24. These AP chains formed less thermally stable AP double helices during retrogradation; however, they melt following the reheating process, thereby becoming more available to the digestive enzymes. The SDS_{rh} fraction was negatively correlated to ACL_{AP1} and RC_{AP2}, and positively correlated with RC_{AP1}, showing that higher amount and shorter AP chains with DP 6–36 led to more SDS after reheating.

4. Conclusions

The retrogradation behavior and RS3 contents of HASs with varying AAC and fine structures were investigated in this study. DSC analysis identified retrograded AP, AM-lipid complexes, and retrograded AM crystals based on their melting temperatures. Notably, as AAC increased to 57 % after one day of storage at 4 °C, a transition from AP to AM retrogradation was observed in these HASs. RS3 content (31.9 % - 50.3 %) did not exhibit a linear increase with increasing AAC but followed the trends of retrogradation extent and structural order, suggesting a greater influence of other structural variations than AAC alone. In contrast, thermally stable RS3 obtained through reheating, varying 18.3 % - 39.5 %, increased with AAC and then plateaued at 57 %. Pearson correlation and PCA analysis further revealed that contents of retrograded AP, AM-lipid complexes, and retrograded AM were positively associated with amount of AP chains with DP 13–24, AM chains with DP 500–5000, and short AM chains with DP < 500, respectively. Additionally, higher structural order was associated with longer AP chains (DP 6–36), a greater proportion of AP chains with DP > 36, and shorter AM chains with DP < 500. Furthermore, RS3 in these HASs comprised a mixture of double-helical and single-helical aggregates, with their levels likely enhanced by increasing AM chains with DP < 5000 and AP chains with DP > 36, although further validation in the future is needed. Based on these findings, we propose a two-step strategy for optimizing RS3: (1) increasing AAC to a relatively high level (e.g., > 57 %) and (2) optimizing the fine structures of AM and AP. Starchy foods with high RS3 can be applied to the diet of diabetics and obese people to lower their postprandial blood glucose levels.

CRediT authorship contribution statement

Li Ding: Writing – original draft, Validation, Software, Methodology, Investigation, Conceptualization. **Jiyu Yang:** Software, Methodology. **Jacob Judas Kain Kirkensgaard:** Writing – review & editing, Methodology. **Kasper Enemark-Rasmussen:** Writing – review & editing, Methodology. **Jinhui Chang:** Writing – review & editing. **Lude Zhang:** Writing – review & editing. **Sheng Chen:** Writing – review & editing. **Andreas Blennow:** Writing – review & editing, Resources. **Yuyue Zhong:** Writing – review & editing, Supervision, Resources, Project administration, Conceptualization.

Declaration of competing interest

The authors declare that they have no known competing financial interests or personal relationships that could have appeared to influence the work reported in this paper.

Acknowledgements

Li Ding wants to thank the China Scholarship Council funding (CSC, 202006150028) supporting her PhD study at the University of Copenhagen, Denmark. Wide-angle X-ray scattering data was produced by the research infrastructure at The Department of Food Science at the University of Copenhagen, partly funded by FOODHAY (Food and Health Open Innovation Laboratory, Danish Roadmap for Research Infrastructure).

Appendix A. Supplementary data

Supplementary data to this article can be found online at https://doi.org/10.1016/j.carbpol.2025.123633.

Data availability

Data will be made available on request.

References

Barclay, A. W., Petocz, P., McMillan-Price, J., Flood, V. M., Prvan, T., Mitchell, P., & Brand-Miller, J. C. (2008). Glycemic index, glycemic load, and chronic disease risk—A meta-analysis of observational studies. *American Journal of Clinical Nutrition, 87*(3), 627–637.

Becker, A., Hill, S. E., & Mitchell, J. R. (2001). Relevance of amylose-lipid complexes to the behaviour of thermally processed starches. *Starch - Stärke, 53*(3–4), 121–130.
Bertoft, E. (2017). *Understanding Starch Structure: Recent Progress. Agronomy, 7*(3), 56.
Blennow, A., Wischmann, B., Houborg, K., Ahmt, T., Jorgensen, K., Engelsen, S. B., & Poulsen, P. (2005). Structure function relationships of transgenic starches with engineered phosphate substitution and starch branching. *International Journal of Biological Macromolecules, 36*(3), 159–168.
Carciofi, M., Blennow, A., Jensen, S. L., Shaik, S. S., Henriksen, A., Buléon, A., & Hebelstrup, K. H. (2012). Concerted suppression of all starch branching enzyme genes in barley produces amylose-only starch granules. *BMC Plant Biology, 12*(1), 223.
Castro-Campos, F. G., Esquivel-Fajardo, E. A., Morales-Sanchez, E., Rodriguez-Garcia, M. E., Barron-Garcia, O. Y., Ramirez-Gutierrez, C. F., … Gaytan-Martinez, M. (2024). Resistant starch type 5 formation by high amylopectin starch-lipid interaction. *Foods, 13*(23).
Chang, F., He, X., & Huang, Q. (2013). The physicochemical properties of swelled maize starch granules complexed with lauric acid. *Food Hydrocolloids, 32*(2), 365–372.
Chang, Q., Zheng, B., Zhang, Y., & Zeng, H. (2021). A comprehensive review of the factors influencing the formation of retrograded starch. *International Journal of Biological Macromolecules, 186*, 163–173.
Chung, H.-J., & Liu, Q. (2009). Impact of molecular structure of amylopectin and amylose on amylose chain association during cooling. *Carbohydrate Polymers, 77*(4), 807–815.
Ding, L., Zhang, B., Tan, C. P., Fu, X., & Huang, Q. (2019). Effects of limited moisture content and storing temperature on retrogradation of rice starch. *International Journal of Biological Macromolecules, 137*, 1068–1075.
Ding, L., Liang, W., Qu, J., Persson, S., Liu, X., Herburger, K., & Zhong, Y. (2023). Effects of natural starch-phosphate monoester content on the multi-scale structures of potato starches. *Carbohydrate Polymers, 310*, Article 120740.
Dobosz, A., Sikora, M., Krystyjan, M., Tomasik, P., Lach, R., Borczak, B., & Lukasiewicz, M. (2019). Short- and long-term retrogradation of potato starches with varying amylose content. *Journal of the Science of Food and Agriculture, 99*(5), 2393–2403.
Gelders, G., Vanderstukken, T., Goesaert, H., & Delcour, J. (2004). Amylose–lipid complexation: A new fractionation method. *Carbohydrate Polymers, 56*(4), 447–458.
Gelders, G. G., Duyck, J. P., Goesaert, H., & Delcour, J. A. (2005). Enzyme and acid resistance of amylose-lipid complexes differing in amylose chain length, lipid and complexation temperature. *Carbohydrate Polymers, 60*(3), 379–389.
Gidley, M. J., & Bulpin, P. V. (1987). Crystallisation of malto-oligosaccharides as models of the crystalline forms of starch: Minimum chain-length requirement for the formation of double helices. *Carbohydrate Research, 161*(2), 291–300.
Gidley, M. J., & Bulpin, P. V. J. M. (1989). Aggregation of amylose in aqueous systems: The effect of chain length on phase behavior and aggregation kinetics. *Macromolecules, 22*(1), 341–346.
Gidley, M. J. J. M. (1989). Molecular mechanisms underlying amylose aggregation and gelation. *Macromolecules, 22*(1), 351–358.
Gomand, S. V., Lamberts, L., Visser, R. G. F., & Delcour, J. A. (2010). Physicochemical properties of potato and cassava starches and their mutants in relation to their structural properties. *Food Hydrocolloids, 24*(4), 424–433.
Gong, B., Cheng, L., Gilbert, R. G., & Li, C. (2019). Distribution of short to medium amylose chains are major controllers of in vitro digestion of retrograded rice starch. *Food Hydrocolloids, 96*, 634–643.
Grewal, N., Faubion, J., Feng, G., Kaufman, R. C., Wilson, J. D., & Shi, Y. C. (2015). Structure of waxy maize starch hydrolyzed by Maltogenic alpha-amylase in relation to its Retrogradation. *Journal of Agricultural and Food Chemistry, 63*(16), 4196–4201.
Guo, K., Liu, S., Zhang, L., Zhang, Q., Yu, Y., Ma, P., & Bian, X. (2024). Influence of elevated potassium fertilization on structural and functional properties of sweet potato root tuber starch. *Foods, 13*(23), 3890.
Gutiérrez, T. J., & Tovar, J. (2021). Update of the concept of type 5 resistant starch (RS5): Self-assembled starch V-type complexes. *Trends in Food Science & Technology, 109*, 711–724.
Han, S. H., Kim, M. J., Lee, S. W., & Rhee, C. (2009). Influence of reheating method and water content on change of the physicochemical properties of retrograded Rice starch. *Starch - Stärke, 61*(9), 520–527.
Haralampu, S. G. (2000). Resistant starch—A review of the physical properties and biological impact of RS3. *Carbohydrate Polymers, 41*(3), 285–292.
Heilbronn, L. K., Noakes, M., & Clifton, P. M. (2002). The effect of high- and low-glycemic index energy restricted diets on plasma lipid and glucose profiles in type 2 diabetic subjects with varying glycemic control. *Journal of the American College of Nutrition, 21*(2), 120–127.
Karim, A. A., Norziah, M. H., & Seow, C. C. (2009). Methods for the study of starch retrogradation. *Food Chemistry, 71*(1), 9–36.
Karunarathna, S., Wickramasinghe, I., Brennan, C., Truong, T., Navaratne, S., & Chandrapala, J. (2024). Investigating the impact of boiling and pressure cooking on resistant starch levels in food. *International Journal of Food Science & Technology, 59*(6), 3907–3917.
Klucinec, J. D., & Thompson, D. B. (1999). Amylose and amylopectin interact in Retrogradation of dispersed high-amylose starches. *Cereal Chemistry, 76*(2), 282–291.
Lafiandra, D., Riccardi, G., & Shewry, P. R. (2014). Improving cereal grain carbohydrates for diet and health. *Journal of Cereal Science, 59*(3), 312–326.
Lii, C.-y., Lai, V. M. F., & Shen, M.-C. (2004). Changes in Retrogradation properties of Rice starches with amylose content and molecular properties. *Cereal Chemistry Journal, 81*(3), 392–398.
Li, C., Hu, Y., Huang, T., Gong, B., & Yu, W. W. (2020). A combined action of amylose and amylopectin fine molecular structures in determining the starch pasting and retrogradation property. *International Journal of Biological Macromolecules, 164*, 2717–2725.
Li, C., Hu, Y., & Li, E. (2021). Effects of amylose and amylopectin chain-length distribution on the kinetics of long-term rice starch retrogradation. *Food Hydrocolloids, 111*, Article 106239.
Li, G., & Zhu, F. (2017). Amylopectin molecular structure in relation to physicochemical properties of quinoa starch. *Carbohydrate Polymers, 164*, 396–402.
Lu, H., Tian, Y., & Ma, R. (2023). Assessment of order of helical structures of retrograded starch by Raman spectroscopy. *Food Hydrocolloids, 134*, Article 108064.
Luckett, C. R., & Wang, Y. J. (2012). Effects of beta-amylolysis on the resistant starch formation of debranched corn starches. *Journal of Agricultural and Food Chemistry, 60*(18), 4751–4757.
Ma, Z., Hu, X., & Boye, J. I. (2020). Research advances on the formation mechanism of resistant starch type III: A review. *Critical Reviews in Food Science and Nutrition, 60*(2), 276–297.
Palacios-Fonseca, A. J., Castro-Rosas, J., Gómez-Aldapa, C. A., Tovar-Benítez, T., Millán-Malo, B. M., del Real, A., & Rodríguez-García, M. E. (2013). Effect of the alkaline and acid treatments on the physicochemical properties of corn starch. *CyTA Journal of Food, 11*(sup1), 67–74.
Park, E. Y., Baik, B.-K., & Lim, S.-T. (2009). Influences of temperature-cycled storage on retrogradation and in vitro digestibility of waxy maize starch gel. *Journal of Cereal Science, 50*(1), 43–48.
Ramdath, D. D., Liu, Q., Donner, E., Hawke, A., Kalinga, D., Winberg, J., & Wolever, T. M. S. (2017). Investigating the relationship between lentil carbohydrate fractions and in vivo postprandial blood glucose response by use of the natural variation in starch fractions among 20 lentil varieties. *Food & Function, 8*(10), 3783–3791.
Schulze, M. B., Liu, S., Rimm, E. B., Manson, J. E., Willett, W. C., & Hu, F. B. (2004). Glycemic index, glycemic load, and dietary fiber intake and incidence of type 2 diabetes in younger and middle-aged women. *The American Journal of Clinical Nutrition, 80*(2), 348–356.
Sievert, D., & Wursch, P. (1993). Amylose chain association based on differential scanning calorimetry. *Journal of Food Science, 58*(6), 1332–1335.
Tan, I., Flanagan, B. M., Halley, P. J., Whittaker, A. K., & Gidley, M. J. (2007). A method for estimating the nature and relative proportions of amorphous, single, and double-helical components in starch granules by 13C CP/MAS NMR. *Biomacromolecules, 8*(3), 885–891.
Tian, Y., Liu, X., Kirkensgaard, J. J. K., Khakimov, B., Enemark-Rasmussen, K., Hebelstrup, K. H., & Zhong, Y. (2024). *Characterization of different high amylose starch granules* (p. 146). Part I: Multi-scale structures and relationships to thermal properties. Food Hydrocolloids.
Tian, Y., Petersen, B. L., Liu, X., Li, H., Kirkensgaard, J. J. K., Enemark-Rasmussen, K., & Blennow, A. (2024). *Characterization of different high amylose starch granules* (p. 149). Part II: Structure evolution during digestion and distinct digestion mechanisms. Food Hydrocolloids.
Vamadevan, V., & Bertoft, E. (2018). Impact of different structural types of amylopectin on retrogradation. *Food Hydrocolloids, 80*, 88–96.
Vandeputte, G. E., Vermeylen, R., Geeroms, J., & Delcour, J. A. (2003). Rice starches. III. Structural aspects provide insight in amylopectin retrogradation properties and gel texture. *Journal of Cereal Science, 38*(1), 61–68.
Villas-Boas, F., Facchinatto, W. M., Colnago, L. A., Volanti, D. P., & Franco, C. M. L. (2020). Effect of amylolysis on the formation, the molecular, crystalline and thermal characteristics and the digestibility of retrograded starches. *International Journal of Biological Macromolecules, 163*, 1333–1343.
Vilpoux, O. F., & Santos Silveira Junior, J. F. (2023). *Global production and use of starch* (pp. 43–66).
Wang, S., Li, C., Copeland, L., Niu, Q., & Wang, S. (2015). Starch Retrogradation: A comprehensive review. *Comprehensive Reviews in Food Science and Food Safety, 14*(5), 568–585.
Wang, S., Wang, S., Guo, P., Liu, L., & Wang, S. (2017). Multiscale structural changes of wheat and yam starches during cooking and their effect on in vitro enzymatic digestibility. *Journal of Agricultural and Food Chemistry, 65*(1), 156–166.
Xu, J., Zhao, W., Ning, Y., Jin, Z., Xu, B., & Xu, X. (2012). Comparative study of spring dextrin impact on amylose retrogradation. *Journal of Agricultural and Food Chemistry, 60*(19), 4970–4976.
You, H., Liang, C., Zhang, O., Xu, H., Xu, L., Chen, Y., & Xiang, X. (2022). Variation of resistant starch content in different processing types and their starch granules properties in rice. *Carbohydrate Polymers, 276*, Article 118742.
Yu, S., Ma, Y., & Sun, D.-W. (2009). Impact of amylose content on starch retrogradation and texture of cooked milled rice during storage. *Journal of Cereal Science, 50*(2), 139–144.
Yu, S., Xu, J., Zhang, Y., & Kopparapu, N. K. (2014). Relationship between intrinsic viscosity, thermal and retrogradation properties of amylose and amylopectin. *Czech Journal of Food Sciences, 32*(5), 514–520.
Zhang, B., Huang, Q., Luo, F.-x., & Fu, X. (2012). Structural characterizations and digestibility of debranched high-amylose maize starch complexed with lauric acid. *Food Hydrocolloids, 28*(1), 174–181.
Zhang, B., Dhital, S., & Gidley, M. J. (2015). Densely packed matrices as rate determining features in starch hydrolysis. *Trends in Food Science & Technology, 43*(1), 18–31.
Zhang, L., Zhao, J., Li, F., Jiao, X., Zhang, Y., Yang, B., & Li, Q. (2024). Insight to starch retrogradation through fine structure models: A review. *International Journal of Biological Macromolecules, 273*(Pt 1), Article 132765.

Zhong, Y., Liu, L., Qu, J., Blennow, A., Hansen, A. R., Wu, Y., & Liu, X. (2020). Amylose content and specific fine structures affect lamellar structure and digestibility of maize starches. *Food Hydrocolloids, 108*, Article 105994.
Zhong, Y., Keeratiburana, T., Kain Kirkensgaard, J. J., Khakimov, B., Blennow, A., & Hansen, A. R. (2021). Generation of short-chained granular corn starch by maltogenic alpha-amylase and transglucosidase treatment. *Carbohydrate Polymers, 251*, Article 117056.
Zhu, B., Zhan, J., Chen, L., & Tian, Y. (2020). Amylose crystal seeds: Preparation and their effect on starch retrogradation. *Food Hydrocolloids, 105*, Article 105805.